RSC Applied Polymers

ROYAL SOCIETY OF CHEMISTRY

REVIEW

View Article Online
View Journal | View Issue

Cite this: *RSC Appl. Polym.*, 2025, **3**, 299

Shear-stiffening supramolecular polymers: fabrication, modification and application

Nan Li, Shiyu Gu, Qi Wu* and Jinrong Wu *

Next-generation flexible protective devices with softer, thinner, and better impact-resistance properties that can meet the extensive and rigorous impact-protection requirements in emerging fields such as aerospace, transportation, and electronics have attracted much attention. Shear-stiffening supramolecular polymers (SSSPs) represent an emerging class of impact-protection materials whose modulus significantly increases with the external strain rate, providing an excellent impact-resistance ability. However, there is still a lack of a comprehensive summary of SSSPs in terms of their aspects ranging from syntheses and structures to modifications and applications. This review outlines the progress in various fabrication approaches, unique properties and mechanisms of SSSPs since the advent of polyborosiloxane. To address their intrinsic cold-flow drawbacks, we provide an overview of the structural stabilization modifications of SSSPs and their subsequent applications in protection, flame retardancy, and sensors. Finally, we discuss the challenges and prospects for the further investigation of SSSPs in impact protection.

Received 16th October 2024,
Accepted 11th December 2024

DOI: 10.1039/d4lp00316k

rsc.li/rscapplpolym

1. Introduction

Over the history of humanity, materials to protect the human body against enemy attacks have evolved, starting from animal skins to wood, stone, copper and steel.[1,2] Currently, advanced soft multilayer fabrics reinforced with rigid metals or ceramics are widely used to protect soldiers, police officers, and other security personnel. As protection targets become broader and more sophisticated in the new emerging fields of aerospace, transportation, electronic equipment, precision instruments, and so on, the protective materials required need to be softer and thinner while offering much better impact-resistance. Therefore, some novel and innovative molecular designs are being created and developed for protection materials to withstand extreme impact conditions. Among these, shear-stiffening materials are a newly rising and attractive representative to provide impact protection, which show a significant increase in modulus as the external strain rate increases.[3,4] In other words, shear-stiffening materials behave like solids under rapid strain variation but revert to a liquid-like state under

College of Polymer Science and Engineering, State Key Laboratory of Polymer Materials Engineering, Sichuan University, Chengdu 610065, China.
E-mail: wuqi57@scu.edu.cn, wujinrong@scu.edu.cn

Nan Li

Nan Li is currently pursuing her master's degree at the College of Polymer Science and Engineering, Sichuan University under the supervision of Prof. Jinrong Wu. She received a bachelor's degree from the College of Materials Science and Engineering, Jiangsu University, China in 2023. Her research interests focus on the design and preparation of smart functional polymers based on boron dynamic chemistry.

Shiyu Gu

Shiyu Gu is currently pursuing her Ph.D. degree at Sichuan University under the supervision of Prof. Jinrong Wu. She received a master's degree (2022) from the College of Polymer Science and Engineering, Sichuan University, and a bachelor's degree (2019) from the School of New Energy and Materials, Southwest Petroleum University. Her research interests focus on boron-containing dynamically crosslinked and functional materials.

slow strain variation or static conditions.[5,6] Such specific force rate-responsive performance suggests their great potential for applications in protective equipment, cushioning structures, and smart wearable devices.[7–10]

Generally, shear-stiffening materials can be fabricated *via* two main methods. The first method is dispersing solid nanoparticles into the polymer solution. Here, the formed material is a shear thickening suspension (shear thickening fluid, STF), which exhibits an equilibrium state with uniformly dispersed particles in the fluid, while it displays a thickened state under the shear effect *via* particle–particle and particle–fluid interactions.[11,12] The second method involves forming weak but abundant supramolecular interactions between polymer chains. The resulting materials exhibit shear-stiffening behavior (shear-stiffening supramolecular polymers, SSSPs), which overcomes the inherent sedimentation of the STF, thereby facilitating long-term storage and usage.[4] With the assistance of dissociation and association of dynamic supramolecular bonds, shear-stiffening polymers flow like a viscous liquid (cold-flow property) under static or low-stress impact conditions but undergo a liquid–rubber–glass transition as the external impact load increases. Once the impact load disappears, SSSPs regain their characteristic cold-flow behavior.[5,13–15]

Polyborosiloxane (PBS) is a well-known SSSP commonly called "silly putty", "bouncing putty" and "dilatant compound", in which boron atoms are introduced into silicone-oxygen chains.[16–19] Due to its fascinating viscoelastic properties, PBS was invented in the 1940s as a substitute to address the shortage of natural rubber during World War II.[20] However, the inherent shape instability and irreversible deformation on a long time scale limited the development of PBS in commercial applications as an elastomer. Thus, for a considerable period, its primary use was in children's toys and teaching presentation tools for educational demonstrations of various deformation processes. Most early studies focused on improving the synthesis strategies and mechanisms of the unique solid–liquid transition behavior of PBS. Up until now, various recipes for preparing PBS have been proposed by Vale,[21] Rubinsztajn,[22] Roy,[23] Wright,[24] and Zinchenko,[25] including the direct condensation reaction between small molecules, the modification of hydroxyl-terminated polydimethylsiloxane (PDMS-OH), and the chain cleavage reaction of polydimethylsiloxane (PDMS) under high temperature. In 2016, Boland *et al.* systematically studied the rheological properties of PBS composites incorporated with graphene, overcoming the inevitable creep under its natural state and providing an effective strategy for improving their stability.[26] Subsequently, many strategies to modify PBS have been gradually exploited to achieve shape stability on a long time scale, such as increasing the dynamic bond density, building stable double networks, and compounding with functional fillers (Fig. 1).

As demonstrated by the above discussion, the modification strategies have effectively addressed the inherent cold flow behavior of PBS, meanwhile the modified PBS with robust structural stability offers the opportunity for applications in various fields. Especially, PBS with excellent anti-impact ability can be used as a buffer to fabricate impact-resistant composites.[27] There are two main ways to introduce PBS into composites: one is by doping PBS into polymeric matrices, such as silicone rubber and ethylene-vinyl acetate copolymer (EVA),[28–30] and the other is by immersing PBS into solutions of polymeric matrices, such as porous polyurethane (PU) foam and Kevlar.[31–34] The resulting PBS-based composites have been investigated as soft, lightweight, high-impact-resistant buffers in diverse structures and devices for protecting humans and equipment. In terms of industry, the D3O® company produced a series of PBS-based commercial products for impact protection in different application fields, such as sports, electronics, workwear, and defence (**https://www.d3o.com**). Furthermore, PBS has been compounded with various conductive fillers (*e.g.*, graphene, carbon black, carbon nanotubes, MXene nanosheets, and metal nanoparticles), and the resulting conductive PBS composites with reversible B–O bond have demonstrated a fast self-healing ability, high electronic response, and

Qi Wu

Qi Wu is an associate research fellow at the College of Polymer Science and Engineering, Sichuan University. He received a bachelor's degree from Zhejiang University in 2014, a master's degree from the University of Chinese Academy of Sciences in 2017, and a doctoral degree from Sichuan University in 2021. His research interests focus on the design and study of impact-resistant elastomers enabled by boron dynamic chemistry.

Jinrong Wu

Jinrong Wu is a professor at the College of Polymer Science and Engineering, Sichuan University. He received a bachelor's degree and a doctoral degree in 2003 and 2008, respectively, from the College of Polymer Science and Engineering, Sichuan University. He studied at Texas Tech University as a visiting student from 2007 to 2008 and at Harvard University as a visiting scholar from 2014 to 2016. His current research involves high-performance, functional, and self-healing elastomers and related theoretical problems of elastomer materials.

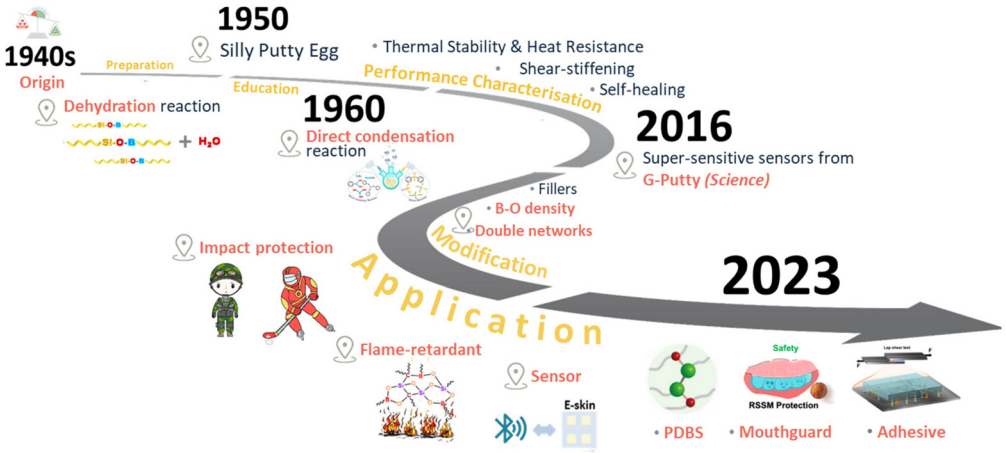

Fig. 1 Graphical representation of the evolution of PBS materials and applications, including super-sensitive sensors made from G-Putty.[26] Copyright 2016, Science. PDBS with a diboron/oxygen bond.[41] Copyright 2023, Springer Nature. Medical mouthguards.[43] Copyright 2024, American Chemical Society. Shear-stiffening bioadhesives.[44] Copyright 2024, American Chemical Society.

excellent skin-attachable performance.[35,36] Such self-healing and conductive PBS composites can elongate the usage time of the materials and have potential for applications in various areas, including electronic skin, wearable electronic devices, human movement monitoring, and medical parameter monitoring.[37–39] In addition, benefiting from the high bonding energy of Si–O–B bonds, PBS can be also used as an efficacious flame-retardant filler for different polymer matrices, such as phenolic resin, polypropylene, and silicone rubber, which can remarkably improve the flame resistance and the smoke suppression performance of the corresponding composites.[29,30]

Especially, our group has focused on PBS-based elastomers for almost a decade, from their fabrications to modifications and applications.[40] To overcome the inherent cold-flow drawbacks of PBS, a covalently crosslinked PDMS network was integrated into a dynamic PBS network, which was then composited with carbon nanotubes to fabricate a sensor with rate-responsive capability.[13] Recently, the diboron structure (B–B) was introduced into the siloxane main chain and utilized to design a novel shear-stiffening material named polydiborosiloxane (PDBS).[41] Compared with traditional monoboron/oxygen dative bonds in PBS, the diboron/oxygen dative bonds in PDBS possessed more abundant coordination forms with more stable bond energies, which enhanced the shear-stiffening effect through a more solid-like state to achieve superior impact-resistance. Based on the excellent anti-impact properties of PDBS, a novel sports mouthguard was developed with a shear-stiffening behavior for the first time, which effectively balanced the opposing demands for good impact-protection ability and a low thickness of the mouthguard.[42,43] Further, a novel silicone-based bioadhesive with shear-stiffening performance was created, whereby it was demonstrated that its cohesive strength increased with the loading rate, thereby realizing a bioadhesive with a rate-response ability and on-demand adhesion capability (Fig. 1).[44]

Overall, supramolecular polymers with shear-stiffening behavior have attracted increasing attention from academia and industry in the past decade as they can exhibit an excellent impact-resistance ability with softness and lightness, thereby satisfying the rigorous demands of impact protection for military equipment, precise instruments, humans, and sportswear. However, there is still a lack of a complete description of SSSPs in a systematic and logical way from their synthesis and structure to modification and application. Consequently, in this review we provide a comprehensive summary of the progress in the various fabrication methods, and describe the unique properties and mechanisms of SSSPs since the advent of PBS. As their inevitable cold-flow feature has limited their more widespread use, we outline the structural stabilization modifications to enhance the stability of SSSPs, as well as broaden their applications in protection, heat resistance, and sensors. Finally, we conclude on the progress to date and present a forward perspective on the outlook for SSSPs and point out the key challenges and potential of SSSP materials for further development, particularly for impact protection.

2. Fabrication methods

PBS was first invented in the 1940s to address the shortage of natural rubber during World War II and involved treating liquid dimethyl siloxane with boric oxide.[20] Subsequently, PBS has been prepared through various pathways to meet the growing demands in different fields. According to existing reports, there are three universally acknowledged strategies to fabricate PBS. The classic method involves a direct condensation reaction between various boron-containing compounds and silicon derivatives (Fig. 2A). Other preparative approaches include the dehydration reaction between hydroxyl groups on boron atoms and PDMS-OH units (Fig. 2B), as well as the

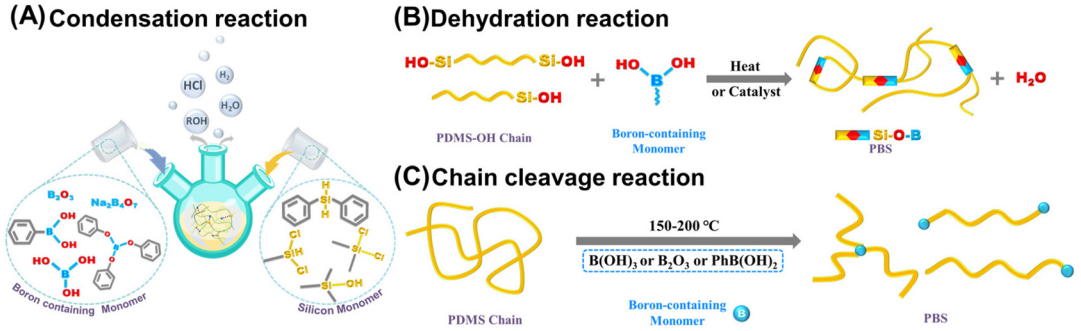

Fig. 2 Fabrication methods for PBS.

chain cleavage reaction of PDMS long chains by boron-containing compounds under high temperatures (Fig. 2C).

2.1 Condensation reaction between silicone and boron-containing monomers

The condensation reaction between boron-containing compounds and organosilicon monomers is the most straightforward method to prepare PBS materials. Generally, organosilicon monomers mainly include organochlorosilanes, organosilanols, organoalkoxysilanes, and other functional siloxanes, while the boron-containing substrates include boric acid, pyroboric acid, boric anhydride, phenylboric acid, borax, boron halides, hydrolyzed esters of boric acid, and alkyl borates.[45] The two main types of condensation reaction applied are direct condensation and hydrolysis condensation (Scheme 1). PBS can be obtained through the direct condensation between boronic acid or boronic esters and chlorosilanes, alkoxysilanes, or silanols, followed by the removal of small molecules such as alcohols, H_2O, HCl, and H_2 (Scheme 1, reactions (1)–(5)). For example, Soraru and co-workers reported the synthesis of PBS materials by directly condensing liquid silicon alkoxide with boric acid ($B(OH)_3$, BA), yielding PBS gels with a high content of Si–O–B bonds after removal of alcohols.[46] Voronkov and Zgonnik mixed BA with alkylchlorosilanes, resulting in different PBS states as viscous liquids or plastic solids.[47] Similarly, Vale's group also added BA to dichlorodimethylsilane, obtaining a transparent viscoelastic PBS product though the release of HCl.[21] In such PBS formation reactions involving releasing small molecule byproducts, the HCl byproduct is considered harmful and can lead to the obtained PBS products containing a high level of halogen residue,[22] while H_2O as a byproduct is detrimental to the integrity of the PBS network and must be removed.

Furtherly, Rubinsztajn's group came up with a simple and environmentally friendly approach for the synthesis of PBS resins involving the dehydrocarbon condensation of trimethyl borate with diphenylsilane and tris(pentafluorophenyl)borane in one pot (Scheme 1, reaction (6)).[22] In 2017, Kuciński and Hreczycho developed a highly chemoselective synthesis method from hydroboranes and silanols, achieving the formation of PBS by a catalyst-free and waste-free dehydrogenative coupling at room temperature (Scheme 1, reaction (7)).[45]

In addition, Andrianov and Volkova investigated the heated reaction of tributyl borate or boron triacetate with organoalkoxysilane, in which condensation occurred with the formation of PBS while butyl or ethyl acetate was eliminated. And as the viscosity of the PBS polymeric product increased, the condensation became slower and could not be completed. Moreover, such copolymerization of boron and silicon species has also been investigated in a sol–gel process involving the hydrolysis and condensation of alkoxides (Scheme 1, reactions (8) and (9)).[48]

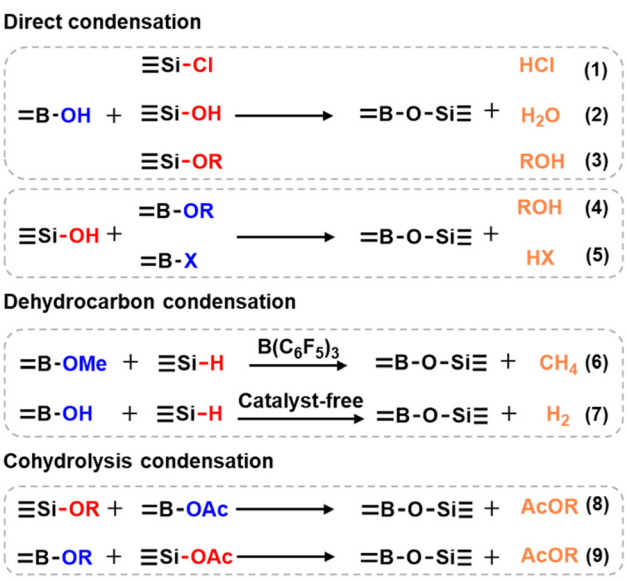

Scheme 1 Different types of methods to prepare PBS. Reaction (6).[22] Copyright 2014, Springer Nature; reaction (7).[45] Copyright 2017, Wiley-VCH Verlag.

2.2 Dehydration reaction between hydroxyl silicone oil and boron-containing small molecules

Another alternative approach for preparing PBS materials is to modify the PDMS-OH with boron-containing small molecules, whereby the polar moieties of the boron terminals facilitate the formation of Si–O–B bonds by grafting onto the unconnected PDMS-OH chain to further promote the dehydration

reaction. To illustrate this, our group combined hydroxyl silicone oil with dichlorfenylmethylsilane and sodium tetraborate ($Na_2B_4O_7$) at 80 °C to create a range of hybrid PBS samples with different B/Si molar ratios, and we found that the viscoelastic properties were influenced by the reversible physical crosslinks *via* weak Si–O : B dative bonds. The temporary splitting and reattachment of the weak Si–O : B bonds in PBS were found to be contingent on the external temperature. As the temperature rose, the physical crosslinks *via* Si–O : B bonds became more susceptible to disruption, reducing the elastic modulus of PBS.[40] Furthermore, Tang *et al.* also prepared PBS by mixing BA and a series of PDMS-OH samples with different molecular masses and investigated the viscoelastic behavior of the formed PBS. The plateau elastic modulus of the PBSs decreased and then increased as the molecular mass of the PDMS precursor increased, as determined by the number density of supramolecular interactions and the topological entanglement.[49] This finding was also confirmed by employing the Doi–Edwards model to study the rheological behavior and relaxation times of reversibly crosslinking PBS materials using the same dehydration reaction.[50] In conclusion, the dehydration reaction between PDMS-OH and boron-containing small molecules is regarded as an easy, viable, and productive approach to obtain PBS materials with an adjustable viscoelastic performance.

2.3 Chain cleavage reaction of polydimethylsiloxane by boron-containing compounds

With the assistance of boron-containing compounds under high temperatures, the silicone-oxygen main chains of PDMS can be cut into segments and linked with boron atoms through B–O–Si bridges, thereby forming PBS materials. For example, McGregor *et al.* added different portions of boron oxide (B_2O_3) into PDMS under temperatures between 100 °C and 250 °C until a coherent rubbery solid was produced. In this reaction, boron oxide was utilized as an effective condensation agent to promote the cleavage of the PDMS chain and facilitate the rearrangement of the Si–O–Si bonds.[23] Further, Wright and co-workers heated PDMS with boron compounds (such as BA, pyroboric acid, boric anhydride, and borate esters) at 150 °C to obtain various types of PBS (bouncing putty). They found that varying the number of boron compounds and the duration of the heat treatment cycles could alter the relative proportions of the hydrophilic and hydrophobic components of the mass, and thus control the degrees of elasticity and plasticity of the obtained bouncing putties.[24]

Based on the above chain cleavage methods, Zinchenko *et al.* investigated the synthetic mechanism and microstructure of PBS. They similarly synthesized PBS at 180–200 °C and determined the structures formed at various stages using IR spectroscopy. It was found that the B–O–Si and B–O–B type groups were formed at temperatures above 150 °C due to the mutual condensation of OH groups attached to the PDMS chains and boric acid.[25] Similarly, Liu *et al.* synthesized PBS materials from PDMS and BA by heating a mixture of these compounds to 200 °C. They found that as random scission of the PDMS chains by BA, the new chain ends were modified by –Si–O–$(BO)_m(OH)_n$ moieties. Further, owing to the abundant hydrogen bonding among the end groups, supramolecular interactions were formed and the dynamic moduli increased dramatically, even though the molecular weight of the PBS was much smaller than that of the original PDMS.[51]

3. Characteristic performance and mechanism

Responsive viscoelasticity is a unique property of PBS materials, in which such materials exhibit viscous and elastic mechanical characteristics depending on the deformation and temperature.[19] Under a long time scale, low strain rate, or high temperature, PBS flows slowly like a viscoelastic liquid, showing typical cold-flow characteristics. Nonetheless, as the applied strain rate gradually increases, the PBS exhibits a solid-like property, undergoing a solid–liquid phase transition from the initial dense state to a rubbery state (Fig. 3A and B).[15,52,53] This unique phenomenon of a cold-flow behavior and solid–liquid property in PBS has been comprehensively researched through experimental analysis and theoretical models. According to the mechanical behaviors of PBS, the stress shows a linear increase with strain at a low strain rate, following a typical viscous liquid behavior. The modulus and viscosity of PBS then increase significantly with the strain rate. When the storage modulus (G') reaches a platform, PBS is transformed from a viscous liquid state to a rubbery state. Subsequently, it exhibits the characteristics of a glassy polymer at a higher strain rate (Fig. 3C and D).[54] Various tests have shown its apparent solid–liquid performance arise by the transition among the liquid-like, rubber-like, and glass-like states with the altering of the applied strain rate.[27,54,55] Furtherly, Cross *et al.* designed a standard linear solid model (SLS) consisting of two springs and a dashpot in series with one of the springs called a Maxwell element. This model provided an excellent qualitative description of the viscoelastic nature of PBS based on the experimental data related to the rapid deformations observed in the dropped mass tests and slow deformation shown by compression measurements (Fig. 3E).[56–59]

Back in the 1960s, boron–oxygen dative bonds between boron atoms and the oxygen atoms in the siloxane backbone were first reported by Wick, who described how these could form dynamic crosslinking and endow PBS materials with shear-stiffening behaviors (Fig. 4A(1)).[25] Subsequently, Juhasz *et al.* developed a model of the microstructure of PBS to furtherly interpret this unique characteristic, whereby the empty sp^3 hybrid orbitals of boron atoms with coordinative unsaturation could favorably form dynamic weak bonds with the free pair of electrons of oxygen atoms in other siloxane chain segments.[19,60] In addition, based on the difference in the source of oxygen atoms, another type of boron–oxygen dative bonding was also reported in PBS materials by Zepeda-Velazquez, in which the boron atoms were coordinated with

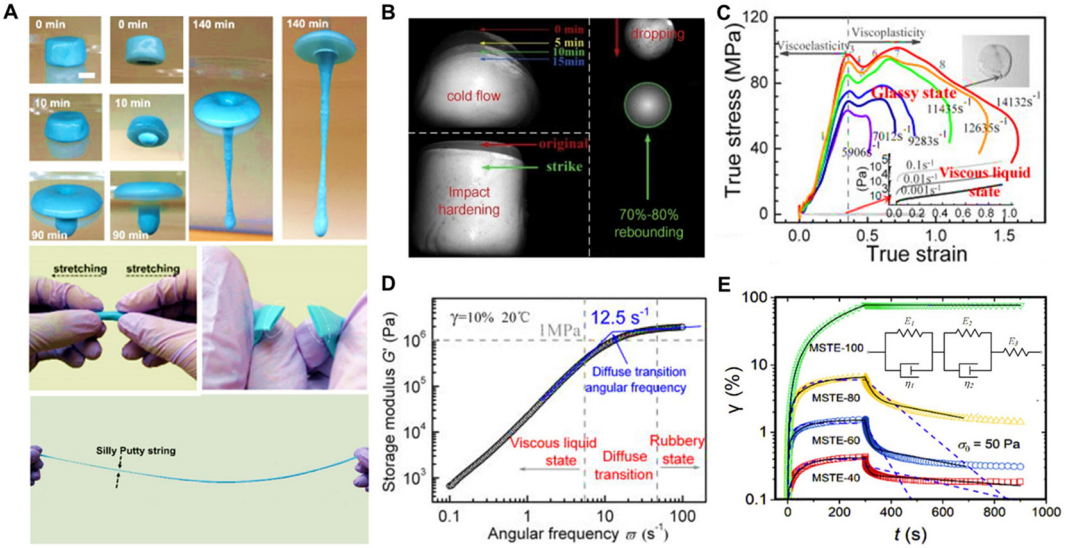

Fig. 3 Characteristics of shear-stiffening properties in PBS. (A) Solid–liquid transition phenomenon of PBS.[52] Copyright 2017, American Chemical Society. (B) Cold-flow behavior of a shear-stiffening polymer composite, impact-induced hardening, and elastic rebound of the shear-stiffening polymer composite.[53] Copyright 2020, Elsevier. (C) Impact-hardening polymer composite's true stress *versus* true strain at high and low strain rates.[54] Copyright 2014, AIP Publishing. (D) Storage modulus of an impact-hardening polymer composite as a function of angular frequency with liquid/solid transition.[54] Copyright 2014, AIP Publishing. (E) Strain curves of magnetorheological PBS in a creep test and the constitutive models based on the SLS model.[59] Copyright 2018, Elsevier.

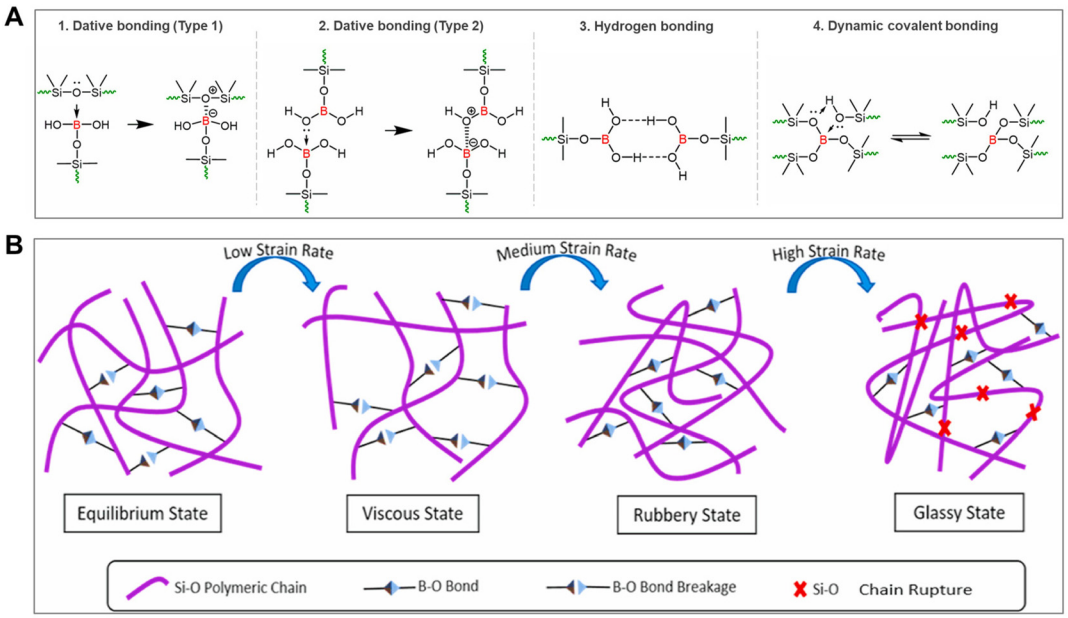

Fig. 4 Mechanism of shear-stiffening properties in PBS. (A) Proposed possible mechanisms of dynamic crosslinking in PBS.[14] Copyright 2023, Elsevier. (B) Mechanism of shear-stiffening behavior among the liquid-like, rubber-like, and glass-like states of PBS.[27] Copyright 2022, Elsevier.

the oxygen atoms on the terminal hydroxyl group of the other PBS chains (Fig. 4A(2)).[61]

Due to the formation of weak supramolecular interaction between the boron and oxygen atoms in boron–oxygen dative bonds, the lone pair of electrons captured by the boron atoms can readily return to the oxygen atoms. At a low strain rate, the B–O dynamic bonds have sufficient time for the processes of fracture and recombination to occur, while the silicone main chains and dynamic crosslinked network can be deformed with slow external force. The entanglement effect between the silicone main chains becomes the primary factor impeding the overall structure deformation, which induces PBS materials to exhibit a liquid-like behavior. At a high strain rate, the dynamic bond relaxation and reconnection rate lag far behind

the external strain changes, which leads to the transient unbroken B–O dynamic bonds creating more prominent resistance against the deformation of the main chains.[15,40,53] Consequently, PBS materials display an elevated stiffness, exhibiting solid-like behavior. Ultimately, once the strain rate exceeds a specific critical value, the Si–O main chains in PBS start to break up, and the second phase transition occurs from the rubbery state to the glassy state (Fig. 4B).[27,50] Furthermore, it was suggested that hydrogen bonding formed by the B–OH groups at the end of the PBS chain likely contributed to the unique viscoelastic nature of PBS materials (Fig. 4A(3)).[51,62] Recently, Bloomfield's group recently proposed another explanation for the viscoelastic property of PBS, which was attributed to the associative exchange of dynamic Si–O–B covalent bonds with neighboring hydroxyl-bearing species (Fig. 4A(4)).[14,137]

Generally, the current explanations for the shear-stiffening effect are mainly based on the dynamic evolution of B–O crosslinking through unique breaking and recovering behaviors. Furthermore, its inherent reversible bonding and dynamic supramolecular network enable PBS to demonstrate an autonomous and repeat self-healing ability. These properties suggest PBS would be an ideal lightweight, soft material for e-skin applications, barrier protection films, and intelligent wearable sensors.

Moreover, the bonding energies of the B–O bond and Si–O bond, which are 537.6 kJ mol^{-1} and 422.5 kJ mol^{-1}, respectively, are much higher than that of the C–C bond (345.6 kJ mol^{-1}).[63–65] In addition, boron atoms can capture electrons from free radicals during combustion to generate a conjugation effect and enable a continuous ceramic surface layer to be formed.[66] Therefore, the partial replacement of silicon atoms in the Si–O main chain with boron atoms could reduce the melting temperature of the ceramic layer and effectively improve the flame retardancy of the composites.[67] In general, such high bond energies of B–O and Si–O bonds endow PBS materials with good thermal stability and heat-resistance performances, thereby providing a platform for their applications in flame-retardant fields.[29,68,69]

4. Structural stabilization modifications

Due to their shape instability and irreversible deformation, PBS materials have been mainly used in children's toys and teaching presentations since the 1940s, which has severely limited the development of their applications in scientific and commercial areas. To widen the application potential, it would be significant to inhibit the creep in the natural state of PBS materials by their structural modification or property regulation. Currently, various burgeoning and accessible strategies have been employed to develop PBS materials with stable structures, which include improving the initial density of the dynamic bonds, constructing stable second networks, and compounding with functional fillers/matrixes (Fig. 5).

4.1 Improvement of the crosslinking density of the supramolecular network

Judging from the above investigations of PBS materials with unique shear-stiffening properties, the distinctive solid–liquid transition effect of PBS materials predominantly depend on

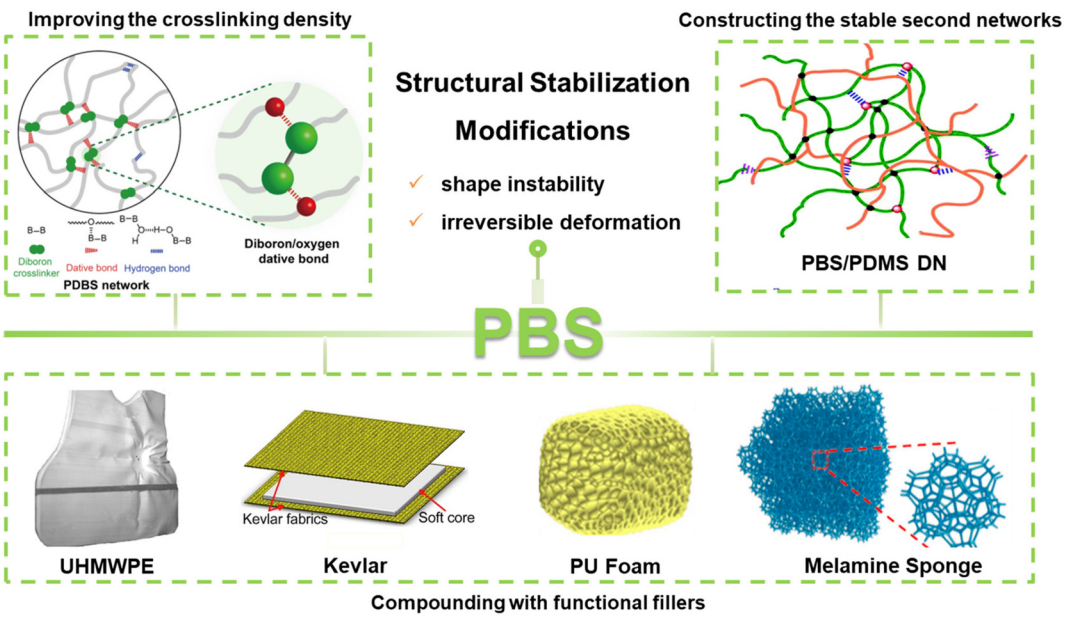

Fig. 5 Illustrations of various modification methods of PBS. Improving the density of dynamic bonds.[41] Copyright 2023, Springer Nature. Building permanent double networks.[70] Copyright 2019, Royal Society of Chemistry. UHMWPE.[71] Copyright 2022, Elsevier. Kevlar fabrics.[72] Copyright 2017, Elsevier. PU foams.[73] Copyright 2022, Elsevier. Melamine sponges.[74] Copyright 2022, American Chemical Society.

the dynamic transition of the crosslinking networks between the boron/oxygen dative bonds within PBS.[75] Therefore, through careful selection of the synthetic monomers, the cold-flow behavior of PBS materials could be controlled by regulating the initial density of the crosslinking network, thus restraining their structure instability. Some investigated strategies are discussed below.

(1) Changing the chain length of PDMS-OH: Tang *et al.* designed a range of PBS materials by embedding boric acid into PDMS-OH with different molecular weights to gain insights into the relationship between the molecular weight of the PDMS-OH precursors and the viscoelasticity of PBS. It was found that the plateau elastic modulus of PBS decreased and then increased with the molecular mass of the PDMS-OH precursors, as determined by FT-IR and dynamic rheological testing, which was collectively associated with the density of the supramolecular interactions and the number density of topological entanglements (Fig. 6A).[49,76] Moreover, Seetapan and co-workers also observed the same trend with a relatively narrow increase in the molecular weight of the PDMS-OH precursor. Thus, adjusting the molecular weight of the PDMS-OH precursor is a kind of modification method for tailoring the viscoelastic properties of PBS materials.[76–78]

(2) Altering the boron concentration of the reactive groups in the boron monomers: Huang *et al.* synthesized a series of PBS materials with different boron contents to reveal the constitutive relationship among the concentration of the combinative boron groups, the density of the dynamic crosslinking networks, and the viscoelastic properties of the PBS materials. Notably, as the boron/silicon ratio increased over the range of 1/300 to 1/3, the relative intensity of the Si–O–B moieties demonstrated an apparent growing tendency, as observed through FT-IR analysis, along with a corresponding two-fold increase in the elastic plateau modulus (Fig. 6B).[40,79] In addition, under high temperature, the growth of the chain segment mobility could cause a breakage of the physical crosslinking between the boron atoms and adjacent oxygen atoms, leading to a decrease in the elastic modulus.[77,80]

(3) Introducing the diboron structure: compared to the monoboron structure, the diboron structure (B–B bond) presents more valence atomic orbitals than valence electrons, thereby manifesting higher electron deficiency. Our group synthesized a novel PBS material (PDBS) by the dehydration reaction between PDMS-OH and diboron acid. Compared with traditional monoboron/oxygen dative bonds in PBS, the diboron/oxygen dative bonds in PDBS possessed a higher bond energy and richer coordination forms (Fig. 6C), which provided a stronger shear-stiffening effect to restrain the chain creep as well as an excellent impact-resistance ability.[41] Taking advantage of this, PDBS materials were investigated as impact-resistant soft substances for use in the dental equipment field.[42,43]

4.2 Construction of a stable second crosslinking network

Even though improving the density of boron/oxygen dynamic crosslinking networks can enhance the structural stability, the obtained PBS materials typically show insufficient structural stability and viscoelasticity over relatively long time scales.[75,83] Therefore, constructing a stable second crosslinking network

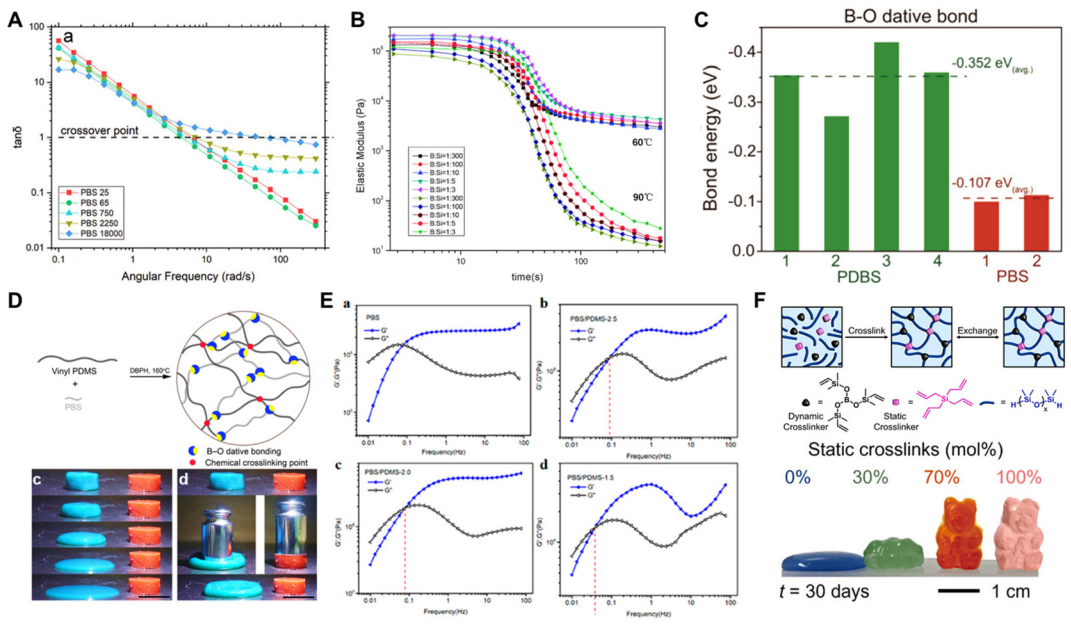

Fig. 6 Structure stabilization modifications of PBS. (A) Tan(δ) curves for PBS materials with different molecular weights.[76] Copyright 2021, John Wiley and Sons. (B) Dynamic time sweep of PBS materials with B/Si molar ratios of 1/300 to 1/3 at 60 °C and 90 °C.[40] Copyright 2014, Royal Society of Chemistry. (C) Bond energy of diboron/oxygen dative bonds in PDBS and PBS.[41] Copyright 2023, Springer Nature. (D) Dual-network construction scheme and photographs of the shape-recovery properties between PBS and samples with the same size.[13] Copyright 2019, American Chemical Society. (E) Rheological measurements of PBS and PBS/PDMS-x.[81] Copyright 2022, American Chemical Society. (F) Scheme for the production of PBS and photographs showing the change in shape over time of the samples.[82] Copyright 2024, American Chemical Society.

is a common way to restrain the cold-flow behavior of the PBS network, further overcoming the inherent structural instability and irreversible deformation of PBS materials. For example, our group introduced a covalently crosslinked PDMS network into a dynamic PBS network, which exhibited high stretchability and satisfactory shape stability over a long time (Fig. 6D).[13] Similarly, Zhu's group also utilized a covalent crosslinking network to stabilize the PBS network. As the proportion of the covalent network increased, the frequency of solid–liquid transformation decreased while the solid-like characteristics of the dual-network elastomer became more prominent (Fig. 6E).[81,84] In addition, a dual-network structure consisting of dynamic PBS and entangled PEG networks was designed by Zhang *et al.* and exhibited excellent mechanical properties with no inherent structural instability.[31,85] Recently, D'Ambra *et al.* synthesized PBS with structural stability *via* the hydrosilylation of chain end- or backbone-functionalized PDMS derivatives with trivinylboronate, whereby a static crosslinking network and the dynamic PBS network were simultaneously formed (Fig. 6F).[82]

4.3 Reinforcement by functional fillers

Compounding with functional materials is also one of the common and effective methods to address the inherent flowability drawbacks of PBS (Fig. 7A), such as adding inorganic-reinforced fillers (carbon nanotubes, MXenes),[32,38,86,87] polymer foams (porous polyurethane foams, melamine sponges),[88,89] and polymer fibers (carbon fibers, Kevlar fabrics, Aramid nanofibers).[27,72,90–95] For example, Chen's group fabricated and compared PBS and its multi-walled carbon nanotube-containing nanocomposites (MWCNT/PBS), and found that the Young's modulus of the nanocomposites significantly increased with the increase of the MWCNT content due to the reinforcement effect of MWCNT (Fig. 7B).[86] Similarly, Chen and Ionov *et al.* overcame the cold-flow drawback of PBS by doping it with graphene, carbon black, and other carbon fillers, which also significantly improved the initial storage modulus of PBS.[85,96,97] Thus, increasing the inorganic-reinforced fillers concentration can result in a higher effect of the crosslinking network on the mechanical performances of blends. In addition, the matrix of the porous network can also be used as a support skeleton to effectively inhibit the cold-flow behavior of PBS. For instance, Fan *et al.* developed novel PBS/PU composites by dip-coating PBS into PU foam, and found its shape could remain stable through the supporting effect provide by the PU (Fig. 7C).[74] Furthermore, the unique 3D porous structure of melamine sponges can also provide stable support for deformable PBS, significantly

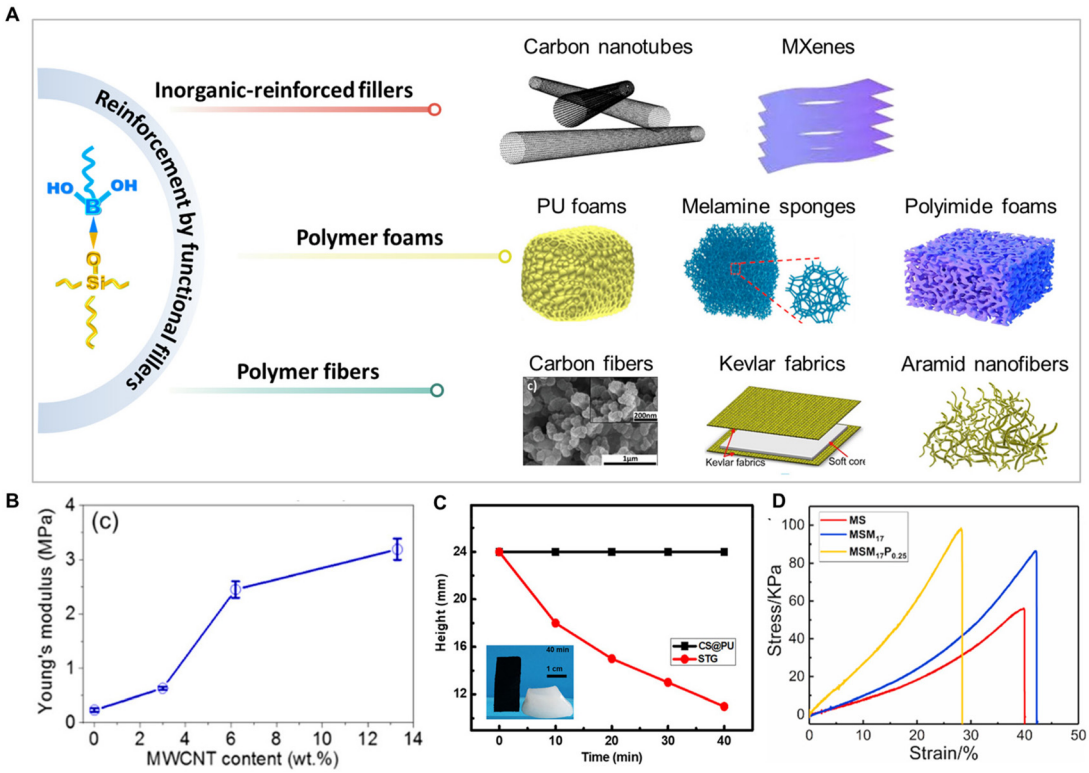

Fig. 7 Functional fillers for PBS. (A) Illustration of the most commonly used composite fillers: PU foams.[73] Copyright 2022, Elsevier. Melamine sponges.[74] Copyright 2022, American Chemical Society. Polyimide foams.[99] Copyright 2023, Elsevier. Carbon fibers.[85] Copyright 2022, Wiley-VCH Verlag. Kevlar fabrics.[72] Copyright 2017, Elsevier. Aramid nanofibers.[100] Copyright 2018, Elsevier. (B) Young's modulus of MWCNT/PBSs with different MWCNT contents.[86] Copyright 2016, American Chemical Society. (C) Shape–Time curves of PBS and PU/PBS samples in a natural state.[74] Copyright 2022, American Chemical Society. (D) Stress–strain curves of melamine/PBS composites.[98] Copyright 2021, Elsevier.

increasing the tensile strength of PBS, and thus effectively solving the cold-flow problem of PBS (Fig. 7D).[98]

5. Application fields

PBS was first prepared in the 1940s and has since been widely used in toys and teaching demonstrations. Due to its inherent shape instability, its application in the industrial field has been minimal to date. In 2016, Boland *et al.* systematically studied the rheological properties of the PBS matrix by adding graphene and published their research in ***Science***, which widely attracted the attention of researchers around the world.[26] Subsequently, the modification and applications of PBS have been extensively researched worldwide. Based on the above discussions of the properties and modifications of PBS, PBS has now been used in personal protective equipment, multifunctional flexible sensors, and heat-resistant materials.

5.1 Impact-protection field

With the ever-increasing demand for safety protection, developing softer, thinner, and much better impact-resistant materials is essential and desirable for military security and personal protection. Inspired by various natural organisms with excellent energy-cushioning structures, such as bee nests,[91] cat paws,[89] cartilage[31] and nacre,[32] several emerging impact-resistant skeleton materials with bioinspired networks or laminates have been developed to create protection for the whole body or vulnerable joints, which is a significant promising strategy in the military, medical, and industrial fields. In particular, PBS materials are considered as ideal candidates for potential applications in smart anti-impact protective devices, and are commonly used as soft material fillers in bioinspired porous skeletons, polymer foams, and polymer fibers due to their shear-stiffening properties. For example, PBS materials used as a buffer for composite laminates have a higher impact energy absorption capacity compared to other traditional cushioning materials, such as chloroprene rubber, ethylene propylene rubber, ethylene-vinyl acetate copolymer, and polyurethane.[27] Therefore, the resulting PBS-based composites have been widely investigated to design soft, lightweight, and high-impact buffer structural components for the protection of humans and equipment.

In the military protection field, designing lightweight and soft safeguards with excellent anti-impact ability has become a prominent research topic, aiming to facilitate the safe mobility of soldiers during military operations and mitigate injuries caused by ballistic impacts.[101,102] According to research, adding a PBS filler to the cushioning layer in body safeguards is an excellent and feasible solution to absorb external impact energy, which could reduce the impact strength experienced by the human body. For example, a smart electronic helmet device was developed by attaching conductive PBS/PU composite foams or PBS/Kevlar fabrics to the helmet liner, which exhibited high efficiency and sensitivity in detecting and simultaneously buffering the impact signals from external impact forces (Fig. 8A).[74]

Typically, body armor is widely employed to protect personnel engaged in military activities, such as soldiers, police officers, and other security personnel, due to its ability to resist or absorb external impact energy. To satisfy the requirements for softer, thinner, and much better anti-impact protection, flexible composite body armor was successfully designed using PBS as a buffer coating in combination with multilayer

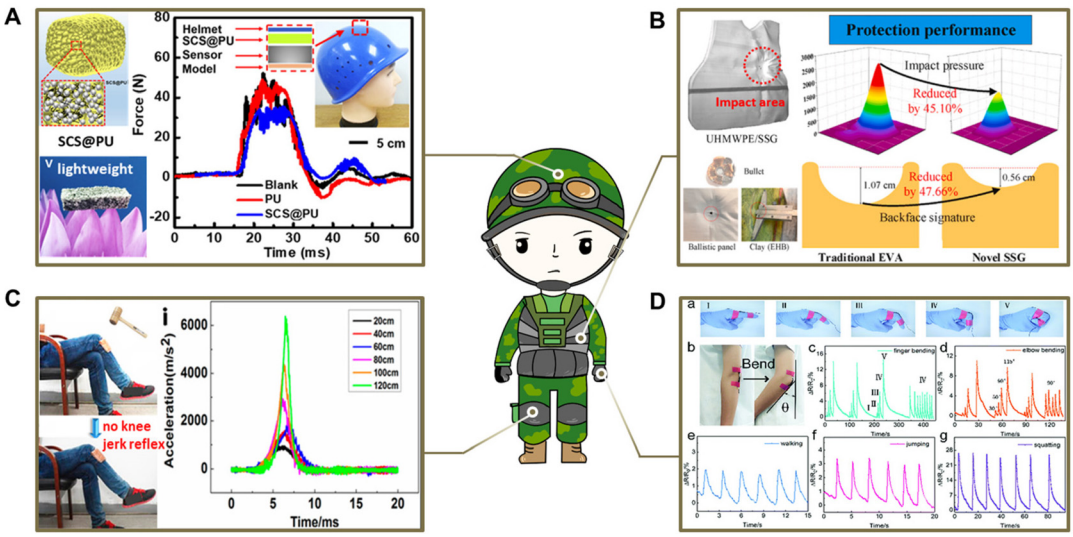

Fig. 8 Protective equipment application of PBS in the military and medical fields. (A) Construction of PBS/PU composite foams and anti-impact properties as a smart helmet liner.[74] Copyright 2022, American Chemical Society. (B) Deformation process and impact pressure distribution of two types of body armor models under ballistic impact experiments.[71] Copyright 2022, Elsevier; (C) knee-jerk reaction testing and dynamic sensing performance of anti-impact knee pads.[88] Copyright 2016, American Chemical Society. (D) Electromechanical performance of a CNTs/PBS-based wrist or elbow guard device.[38] Copyright 2019, Royal Society of Chemistry.

ultrahigh-molecular-weight polyethylene (UHMWPE) ballistic plates to fully absorb the external impact forces, which could effectively disperse the impact energy around the impact area and reduce the maximum impact force by about 4 times compared to a neat UHMWPE ballistic plate (Fig. 8B).[71]

Furthermore, the impact energy absorption capacity of the PU matrix was also significantly enhanced by compounding the PBS into a flexible PU sponge. It was demonstrated that the obtained PU sponge-based impact-resistant composite could be used as an intelligent wearable knee pad for training protection (Fig. 8C).[88] Notably, the conductive CNTs/PBS matrix could also be impregnated in Kevlar fabrics to form a flexible wearable device for protection of the hands or elbows, effectively cushioning 70.5% of impact energy and enabling tracking the body's joints during movement (Fig. 8D).[38]

PBS composites have also attracted considerable attention in recent years in the medical field as a potential strategy to develop lightweight, flexible, and comfortable protective devices, due to their intelligent impact-resistant ability. Based on the shear-stiffening effect, our group developed a novel shear-stiffening mouthguard (SSM) by blending PDBS with diboron/oxygen dative bonds, PDMS, and silica nanoparticles. The SSM exhibited a significant enhancement in shock-absorption capability with a reduction in peak force of approximately 60% and an increase in buffer time of about three-fold compared to commercial mouthguard materials (Fig. 9A). The average Young's modulus of SSM was lower than that of commercial mouthguards, while also possessing both an excellent shock-absorption capability and softer perception. This showed they could be used to protect oral tissues while simultaneously improving the wearability of the mouthguard (Fig. 9B).[42]

In addition, PBS materials have been employed innovatively to safeguard or rectify other vulnerable joints in the body, thus preventing discomfort, injury, and even mortality resulting from collisions and violent impacts. For example, Liang and co-workers developed core–shell high-impact nanofibers with a PBS-filled core assembled into a micron-sized thickness,

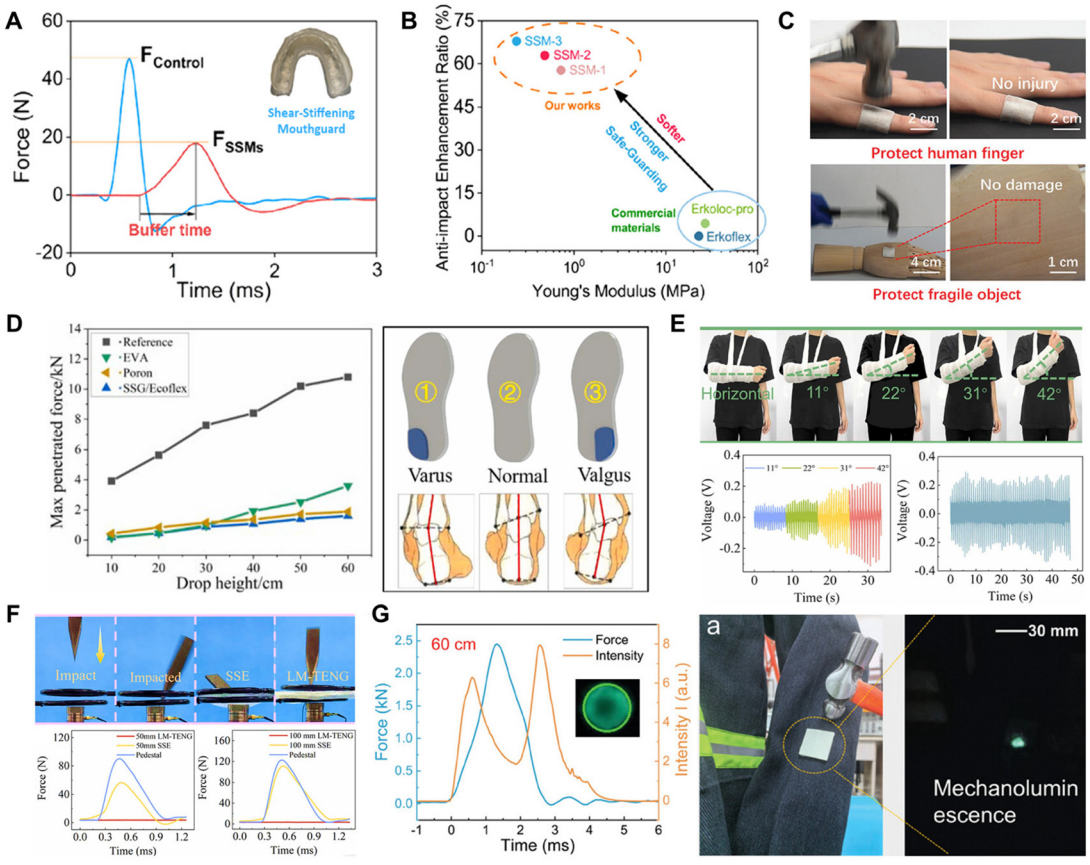

Fig. 9 Impact-resistant wearable devices in medical and industrial applications. (A) Illustration depicting the peak force and the buffer time and anti-impact enhancement ratio.[42] Copyright 2023, American Chemical Society. (B) Elastic modulus and anti-impact reinforcement ratio of SSMs and commercial mouthguard materials.[42] Copyright 2023, American Chemical Society. (C) Smart nanofibers that can provide protection for human fingers and fragile objects.[103] Copyright 2024, John Wiley and Sons. (D) Anti-impact tests of different insoles and corrective images of PBS-based insoles for pronated and ectopic feet.[104] Copyright 2021, Elsevier. (E) Comparison of the anti-impact properties from sharp objects between SSE and smart medical plasters at different fall heights.[105] Copyright 2023, Elsevier. (F) Smart medical plaster possessing stable self-powered sensing capabilities during patient elbow flexion movements.[105] Copyright 2023, Elsevier. (G) Distribution of impact force and corresponding light intensity over time for PBS materials, and their attachment to clothing surfaces for impact visualization.[107] Copyright 2024, John Wiley and Sons.

which could effectively attenuate impact forces to protect human fingers (Fig. 9C).[103] Furthermore, kneecaps or sports insoles equipped with the multi-performance PBS composite could resist external impact while detecting motion signals. In particular, sports insoles could buffer the dynamic impact of the foot during exercise while also physically correcting an abnormal walking gait (Fig. 9D).[104] Recently, Gong *et al.* developed a smart medical plaster with self-powered sensing and anti-impact performance by combining a liquid alloy (LM) with a PBS matrix. The LM phase transition resulting from the Joule heat effect enabled the plaster to soften in response to the applied voltage, thereby facilitating the casualty with the ability to move freely while maintaining stable self-powered sensing capabilities, allowing doctors to continuously monitor the movement and recovery of the patient in real-time (Fig. 9E). Significantly, the plaster demonstrated effective anti-impact properties from sharp objects penetration loading, considerably contributing to human fracture rehabilitation research (Fig. 9F).[105] Further, they introduced mechanoluminescent materials into PBS to visually clarify the impact injuries and enable warnings to be issued in real-time. Therefore, the PBS materials provide a potential pathway to design protective devices with an impact visualization ability (Fig. 9G).[106,107] Recently, D3O® has been introduced with PBS into polyurethane to industrially produce a wide range of impact-protection products, such as helmets, knee guards, vests, and chest protectors. These commercial products not only provide protection for soldiers, athletes, and workers, but also a series of protective films have been produced for the protection of industrial equipment and electronic products in sports and industry (**https://www.d3o.com**).

Typically, these multifunctional wearable protective products require a combination of multiple specific properties to meet the growing demands in applications, such as sensitive dynamic sensing performance, stable thermal conductivity, and high electromagnetic interference (EMI) shielding ability. Thus, incorporating PBS into composite materials can endow the materials with the anti-impact property, while simultaneously protecting other fillers (*e.g.*, graphene and MXenes) from external impact damage to maintain other special functions of the products.[73,98]

5.2 Self-healing field

It is well known that PBS is a kind of supramolecular elastomer exhibiting fascinating intrinsic self-healing properties due to the dynamic association/dissociation of the boron/oxygen dative bonds, which facilitate its application in multifunctional devices requiring an instantaneous self-healing property.[108,109] For example, Wu *et al.* synthesized MWCNT-reinforced PBS nanocomposites with self-healing capabilities, where their conductive healing efficiency reached 98% after 10 s at room temperature. The conductive nanocomposites were adhered to a flexible PDMS substrate to form a high-performance conductor with an LED. With the assistance of the self-healing performance, the circuit could maintain stable conductivity *via* the light intensity feedback of the LED after performing bending and folding motions (Fig. 10A).[86] Similarly, Narumi *et al.* combined MWCNTs-PBS and common soft materials (polyester fabrics and silicone) to build self-healing devices, including a wearable transformative soft controller, reconfigurable pneumatic soft actuator, healing heart with embedded LEDs, and healable rose puzzle (Fig. 10B).[110] In addition, Xie *et al.* utilized dynamic borate ester bonds and B–O dative bonds to effectively restore the mechanical and stress-luminescence properties of a PBS-based composite after fracture. The tensile strength of this composite could be 75% restored within 10 min at room temperature, and demonstrated a mechano-to-photon conversion capability with a

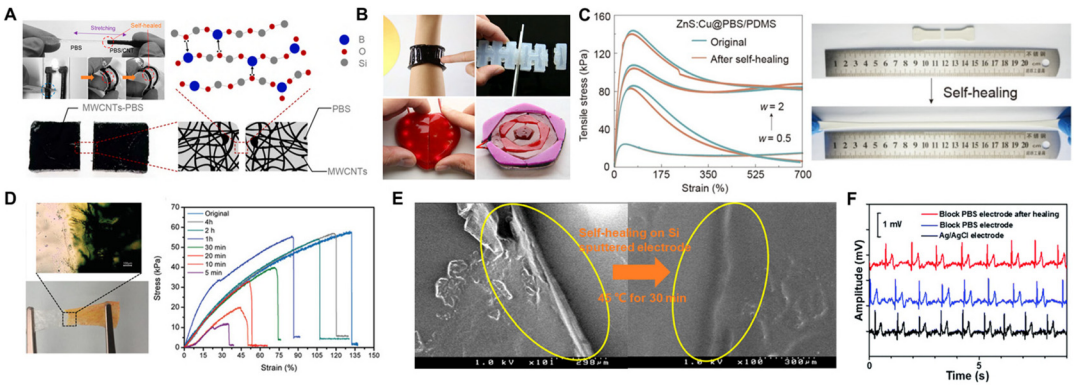

Fig. 10 Self-healing property of PBS. (A) Self-healing mechanism of the MWCNT-PBS composite based on the dynamic crosslinking of boron/oxygen bonds[110] and self-healing as monitored by the light intensity feedback of an LED after bending and folding.[86] Copyright 2019, ACM; 2016, American Chemical Society. (B) Examples of applications of MWCNT-PBS composites, including wearable transformative soft controllers, reconfigurable pneumatic soft actuators, healing hearts with embedded LEDs, and healable rose puzzles.[110] Copyright 2019, ACM. (C) Stress–strain curves and pictures of samples before and after restoration.[111] Copyright 2023, Springer Nature. (D) Stress–strain curves of samples at different restoration durations, and pictures of healed sections.[84] Copyright 2020, John Wiley and Sons. (E) SEM image demonstrating the self-healing property of PBS on the electrode surface.[112] Copyright 2021, American Chemical Society. (F) Electrocardiograms of the electrocardiogram signal acquired before and after injury at a block PBS electrode compared to a commercial Ag/AgCl electrode.[113] Copyright 2022, Royal Society of Chemistry.

maximum efficiency of nearly 100% (Fig. 10C).[111] Similarly, Zhu's group designed reversible imine bonds and dynamic B–O bonds in PDMS to promote the rapid self-healing of cut sections without external stimuli, achieving 98% healing efficiency within 4 h at room temperature, indicating the PDMS elastomers had been endowed with excellent self-healing properties (Fig. 10D).[84]

Recently, Patnaik and co-workers applied PBS solution directly to the electrode surface, and due to the reconnection vie B–O dative bonds, mechanical scars on the electrode surface could be almost completely healed within 30 min, and recovered more rapidly at high temperatures. Such work further extended the application of PBS in self-healing electronic coatings (Fig. 10E).[112] Tang *et al.* designed a novel PBS-based e-skin with fast self-healing properties, which could recover 100% of its original mechanical properties within only 30 s at room temperature after damage, and could even completely recover in 2 min at an ultralow temperature of −20 °C. Furthermore, they doped silver flakes into the above composite to prepare a self-healing PBS-based electrode. They found that the electrocardiogram signal of the cut electrodes could rapidly return to its normal baseline within a few seconds due to the self-healing capacity of the PBS network (Fig. 10F).[113]

5.3 Flame-retardant field

As a typical silicone-based flame retardant, polysiloxanes exhibit excellent thermal stability, flame retardancy, smoke suppression, and environmentally friendly properties due to their Si–O main chain with a high bonding energy.[114,115] To meet the growing demand for highly heat-resistant and flame-retardant safeguarding equipment, introducing heat-resistant hetero atoms or groups is an effective strategy.[116] Notably, PBS is a class of polysiloxane obtained by replacing part of the silicon atoms with boron atoms, which could remain stable under thermal oxidation at 1000 °C.[117,118] This endows PBS with outstanding heat resistance, allowing it to be employed as a flame-retardant component in polymeric materials.

On the one hand, the B–O bonds in PBS have a higher bond energy than Si–O bonds, and the combination of boron–oxygen dative bonds reinforces the interaction between the main chains.[29,68,69] Therefore, PBS was reported to be stable at 500–600 °C and provided nearly 50% char residue at 900 °C, demonstrating robust thermal stability properties of PBS (Fig. 11A).[119] Karagoz and co-workers designed a PBS-based coating with a core–shell structure consisting of a polysiloxane resin core encapsulated by PBS, which served as a heat-resistant adhesive shell (Fig. 11B). This innovative coating exhibited remarkable thermal stability, remaining stable at temperatures up to 600 °C. Such excellent thermal resistance could be primarily attributed to the high bond energies of Si–O–B linkages within the PBS shell.[67,69]

On the other hand, PBS can block the degradation mode of Si–O chains through the cleavage process of cyclic oligomers, thereby generating silyl radicals and Si–H bonds.[120,121] Such a new degradation mode of Si–O chains could effectively promote the rapid charring of the composite to construct crosslinking networks comprising Si–O–Si and Si–O–B structures, which could enhance the oxidation resistance of the surface carbon particles.[120–122] Therefore, the introduction of PBS increased the density of the char layer, which tended to

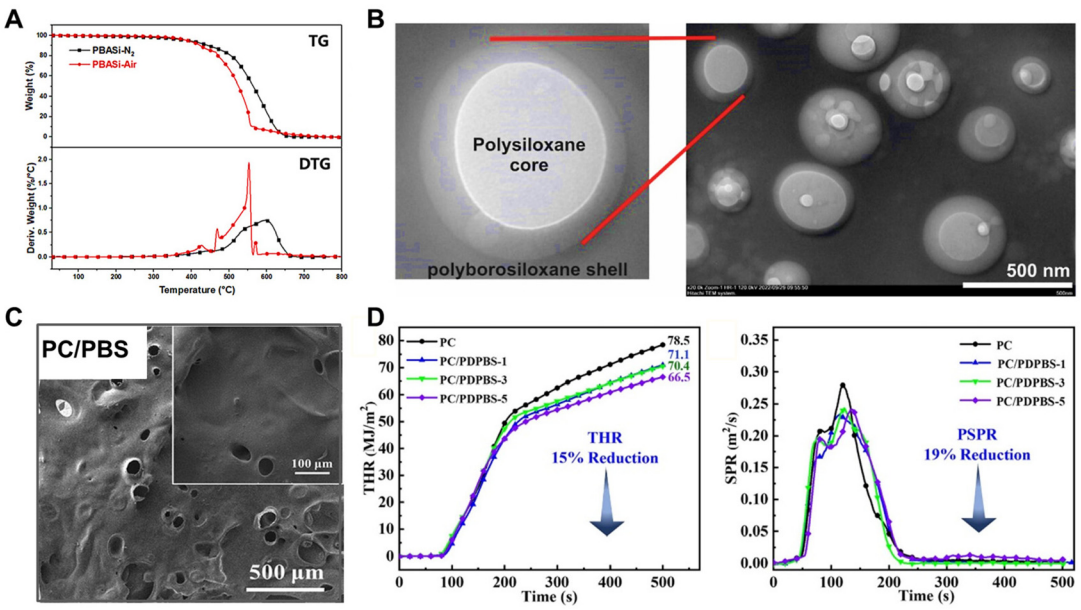

Fig. 11 Mechanism of shear-stiffening properties of PBS. (A) TGA and DTG tests of PBS in air and nitrogen atmospheres.[125] Copyright 2022, Elsevier. (B) TEM images of PBS coatings with a core–shell structure held at 600 °C for 2 h.[69] Copyright 2022, American Chemical Society. (C) SEM image of residual chars after burning.[126] Copyright 2023, Elsevier. (D) THR and SPR values of polycarbonate composites containing PBS in UL-94 tests.[126] Copyright 2023, Elsevier.

form a dense and continuous silicon-boron ceramic-like structure that was attached to the composites during the combustion process (Fig. 11C).[119,123,124] Wang and Tang *et al.* demonstrated that PBS-containing polycarbonate composites could form a laminated structural char layer during the burning process, which drastically reduced the heat release and smoke production rates, thereby enhancing the flame retardancy and smoke suppression of composites (Fig. 11D).[125,126]

5.4 Sensing field

With the development of flexible sensor devices, the requirements for high sensitivity, stability, and a self-healing capability of the sensing substrate materials have attracted considerable research attention. Compared with conventional metal-based and ceramic-based sensors, conductive PBS-based flexible sensors possess low density, high response, and fantastic adhesion, excellent self-healing, and anti-impact properties, which make them promising candidates for potential applications in wearable electronic devices, intelligent soft robots, and medical parameter monitoring.[85,127] An early conductive PBS-based sensor with extreme electromechanical sensitivity was designed by doping conductive graphene into a PBS matrix, which broke through the application limitation of PBS and enabled it to capture the crawling impact of a tiny spider of about 20 mg (Fig. 12A).[26] Subsequently, a series of sensors based on the PBS matrix have been developed, such as piezoelectric sensors,[128] triboelectric sensors,[129,130] gas sensors,[96] strain sensors[131] and liquid metal sensors.[132] For example, Huang's group combined PBS with conductive Ag fillers to enable the highly stable monitoring of biopotential signals under static and dynamic conditions. Based on this design, the solid–liquid characteristics of PBS can ensure that the composite material can maintain stable contact with the monitor's skin without interference from movement and sweat, which is conducive to the real-time diagnosis of biological health conditions and human–computer interactions (Fig. 12B).[133]

Recently, PBS with high moldability, excellent skin-attachability, and fast self-healing properties and its development as a substrate material for electronic skin (e-skin) has become a hot research topic. In this line of study, a multifunctional skin-like substrate based on polymer maltose PBS (PM PBS) was successfully developed. The PM PBS/Ecoflex matrix could be assembled with silver nanowires to form a reusable e-skin that could monitor human movement parameters. Furthermore, it could also be mixed with a piezoelectric filler (PVDF-TrFE) to attach to a tactile sensing gripper arm (Fig. 12C).[134] In addition to detecting various movements of the human body, such as speaking, stroking, and bending, the e-skin also exhibited outstanding thermal responsive properties like a chameleon skin by incorporating thermochromic nanofillers, which facilitated estimation of the environment temperature in real-time based on the e-skin color (Fig. 12D).[135]

In addition, the e-skin obtained by filling the conductive PBS matrix into pressure memory polyurethane foams enabled sensing the occurrence and disappearance of pain like natural human skin (Fig. 12E).[136] Recently, the growing demand for smart wearable devices for use in complex environments has driven the multifunctional development of PBS-based sensors with high sensitivity and high signal resolution to distinguish different stimuli in complex multi-field environments.[129] Fu *et al.* developed a novel composite material by coating PBS on conductive Kevlar fabric. The composite was then attached to the human neck as a strain sensor to trace the venous pulse in real-time, showing a fast response time of 69 ms and a strain resolution better than 0.05% (Fig. 12F).[37] Moreover, PBS composites incorporating highly conductive MXene nanosheets

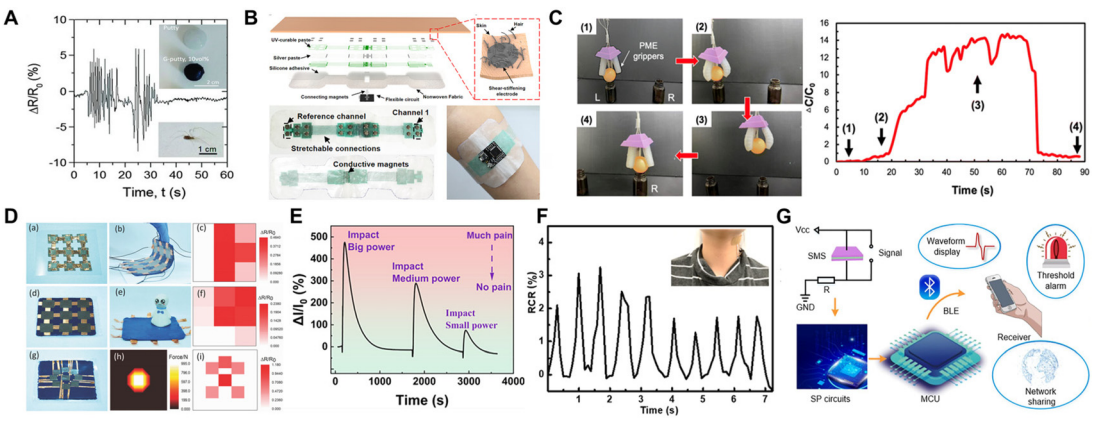

Fig. 12 Application of PBS-based composites in sensing equipment. (A) Change in resistance of a spider as it walked on a G-putty sheet.[26] Copyright 2016, Science. (B) Image of a sensor prepared with PBS as a flexible substrate.[133] Copyright 2024, American Chemical Society. (C) Moving a table tennis ball using a self-healing soft pneumatic gripper and its capacitance value over time.[134] Copyright 2024, Royal Society of Chemistry. (D) Distribution of bending force, static pressure, and dynamic impact sensing and resistance by an e-skin mapping array.[135] Copyright 2018, Wiley-VCH Verlag. (E) PBS-based sensor simulating human skin's response and recovery curve after sensing different impact forces.[136] Copyright 2023, American Chemical Society. (F) PBS-based strain sensors monitoring venous pulse signals in the human neck.[37] Copyright 2022, Elsevier. (G) Schematic of a wireless sensing system based on PBS/MXene sensors.[73] Copyright 2022, Elsevier.

can serve as ideal wearable sensors to monitor human motion data of the human body, such as jumping, bending, and impacts, which offer the potential to utilize artificial intelligence and monitor human–computer interactions. Taking advantage of this, an intelligent wireless sensor system was developed as an early warning device for safety protection, which was capable of responding to impacts promptly and sounding an alarm to keep the human body away from external risks that might cause injuries (Fig. 12G).[73]

6. Conclusions and perspectives

Shear-stiffening supramolecular polymers, especially PBS, possess low weight, high response, excellent skin-attachable properties, fast self-healing capabilities, and anti-impact properties, which suggests their great potential in the design of next-generation intelligent, flexible protection devices. Based on its unique properties and considerable application prospects, various fabrication and modification strategies have been gradually exploited to overcome the inherent structural instability and inevitable cold-flow behavior of PBS. In summary, we comprehensively summarized the recent advances in SSSP materials since the advent of PBS, including the fabrication techniques, unique properties of the materials, underlying mechanisms, modification approaches, and practical applications in protection, self-healing, flame retardancy, and sensing.

Despite the extensive utilization of modified SSSP composites in various fields due to their shear-stiffening properties, there remain considerable challenges and obstacles to designing supramolecular materials with superior multifunctions that can meet the rigorous demands for impact protection in the military, aerospace, and electronic fields; the main aspects are highlighted below.

(1) The current fabrication and modification strategies for SSSPs primarily focus on constructing monoboron dynamic networks on polymer chains, which have limited structural stability and viscoelasticity over relatively long time scales. In response to the increasing need for protection, establishing more stable B–O dynamic networks, such as diboron/oxygen structures, would be an effective approach to enhance the impact-resistance property of materials.

(2) The construction of permanent crosslinking networks or compounding with functional fillers can achieve a better structural stability of SSSPs, but restricts the tunability of the network structure and diminishes the shear-stiffening ability, thereby potentially resulting in insufficient long-term cushioning and protection. Thus, the copolymerization or grafting of Si–O–B structures into covalently crosslinked networks is posited as a viable strategy for maintaining both the structural stability and shear-stiffening properties.

Therefore, with the advent of the smart and high-precision era, the shear-stiffening behavior of SSSPs has attracted dramatically increasing attention from the scientific and industrial communities. The design of new SSSP materials and the enhancement of their shear-stiffening behavior are still big challenges, and much effort should be made to improve these.

Data availability

No primary research results, software or code has been included and no new data were generated or analyzed as part of this review.

Conflicts of interest

The authors declare no competing financial interest.

Acknowledgements

This work was supported by the National Natural Science Foundation of China (52203064 and 52373061).

References

1 S. Siengchin, *Def. Technol.*, 2023, **24**, 1–17.
2 S. Feli and M. R. Asgari, *Composites, Part B*, 2011, **42**, 771–780.
3 R. Mari, R. Seto, J. F. Morris and M. M. Denn, *J. Rheol.*, 2014, **58**, 1693–1724.
4 S. Wang, W. Jiang, W. Jiang, F. Ye, Y. Mao, S. Xuan and X. Gong, *J. Mater. Chem. C*, 2014, **2**, 7133–7140.
5 Y. Wang, X. Gong and S. Xuan, *Smart Mater. Struct.*, 2018, **27**, 065008.
6 C. Clavaud, A. Bérut, B. Metzger and Y. Forterre, *Proc. Natl. Acad. Sci. U. S. A.*, 2017, **114**, 5147–5152.
7 R. C. Neagu, P.-E. Bourban and J.-A. E. Månson, *Compos. Sci. Technol.*, 2009, **69**, 515–522.
8 J. Liang and X.-H. Zhang, *J. Mater. Civ. Eng.*, 2015, **27**, 04014250.
9 X.-G. Lin, F. Guo, C.-B. Du and G.-J. Yu, *Adv. Mater. Sci. Eng.*, 2018, 2018, 2681461.
10 S. Gürgen, M. C. Kuşhan and W. Li, *Prog. Polym. Sci.*, 2017, **75**, 48–72.
11 M. M. Denn, J. F. Morris and D. Bonn, *Soft Matter*, 2018, **14**, 170–184.
12 J. Morris, *Annu. Rev. Fluid Mech.*, 2020, **52**, 121–144.
13 Q. Wu, H. Xiong, Y. Peng, Y. Yang, J. Kang, G. Huang, X. Ren and J. Wu, *ACS Appl. Mater. Interfaces*, 2019, **11**, 19534–19540.
14 A. Kurkin, Y. Lekina, D. G. Bradley, G. L. Seah, K. W. Tan, V. Lipik, J. V. Hanna, X. Zhang and A. l. Y. Tok, *Mater. Today Chem.*, 2023, **33**, 101677.
15 W. Jiang, X. Gong, S. Wang, Q. Chen, H. Zhou, W. Jiang and S. Xuan, *Appl. Phys. Lett.*, 2014, **104**, 121915.
16 R. J. Wojtecki, M. A. Meador and S. J. Rowan, *Nat. Mater.*, 2011, **10**, 14–27.

17 P. Cordier, F. Tournilhac, C. Soulié-Ziakovic and L. Leibler, *Nature*, 2008, **451**, 977–980.
18 M. Goertz, X. Y. Zhu and J. Houston, *J. Polym. Sci., Part B: Polym. Phys.*, 2009, **47**, 1285–1290.
19 A. Juhász, P. Tasnádi and L. Fábry, *Phys. Educ.*, 1984, **19**, 302.
20 A. Christina, T. Diane and G. Peter, *Phys. Educ.*, 2002, **37**, 516.
21 R. L. Vale, *J. Chem. Soc.*, 1960, 2252–2257.
22 S. Rubinsztajn, *J. Inorg. Organomet. Polym. Mater.*, 2014, **24**, 1092–1095.
23 M. R. Roy and E. L. Warrick, *US Pat.*, US2431878A, 1947.
24 J. G. E. Wright, *US Pat.*, US2541851A, 1944.
25 G. A. Zinchenko, V. P. Mileshkevich and N. V. Kozlova, *Polym. Sci. U.S.S.R.*, 1981, **23**, 1421–1429.
26 C. S. Boland, U. Khan, G. Ryan, S. Barwich, R. Charifou, A. Harvey, C. Backes, Z. Li, M. S. Ferreira, M. E. Möbius, R. J. Young and J. N. Coleman, *Science*, 2016, **354**, 1257–1260.
27 K. Myronidis, M. Thielke, M. Kopeć, M. Meo and F. Pinto, *Compos. Sci. Technol.*, 2022, **222**, 109395.
28 F. Ren, Q. Xu, Z. Zhou, W. Xu and H. Ma, *Silicon*, 2020, **12**, 2203–2210.
29 H.-Y. Zhao, J.-B. Zhao, H. Li and T. Zhao, *Chin. J. Polym. Sci.*, 2014, **32**, 187–196.
30 X. Lai, X. Zeng, H. Li and H. Zhang, *J. Macromol. Sci., Part B*, 2014, **53**, 721–734.
31 J. Cheng, Z. Zhang, K. Liu, C. Ma and G. Zhang, *Cell Rep. Phys. Sci.*, 2023, **4**, 101289.
32 S. Liu, S. Wang, M. Sang, J. Zhou, J. Zhang, S. Xuan and X. Gong, *ACS Nano*, 2022, **16**, 19067–19086.
33 S. Zhang, S. Wang, Y. Wang, X. Fan, L. Ding, S. Xuan and X. Gong, *Composites, Part A*, 2018, **112**, 197–206.
34 S. Li, Q. Fu, K. Qian, K. Yu, H. Zhou, Y. Weng and Z. Zhang, *Mater. Des.*, 2020, **195**, 109039.
35 Y. Shen, Z. Lin, X. Liu, T. Zhao, P. Zhu, X. Zeng, Y. Hu, R. Sun and C.-P. Wong, *Compos. Sci. Technol.*, 2021, **213**, 108942.
36 Y.-J. Wan, X.-Y. Wang, X.-M. Li, S.-Y. Liao, Z.-Q. Lin, Y.-G. Hu, T. Zhao, X.-L. Zeng, C.-H. Li, S.-H. Yu, P.-L. Zhu, R. Sun and C.-P. Wong, *ACS Nano*, 2020, **14**, 14134–14145.
37 T. Fan, Z. Sun, Y. Zhang, Y. Li, Z. Chen, P. Huang and S. Fu, *Composites, Part B*, 2022, **242**, 110106.
38 F. Yuan, S. Wang, S. Zhang, Y. Wang, S. Xuan and X. Gong, *J. Mater. Chem. C*, 2019, **7**, 8412–8422.
39 Y. Li, Y. A. Samad, T. Taha, G. Cai, S.-Y. Fu and K. Liao, *ACS Sustainable Chem. Eng.*, 2016, **4**, 4288–4295.
40 X. Li, D. Zhang, K. Xiang and G. Huang, *RSC Adv.*, 2014, **4**, 32894–32901.
41 Q. Wu, Y. Peng, H. Xiong, Y. Hou, M. Cai, Y. Wang, L. Zhao and J. Wu, *Sci. China Mater.*, 2023, **66**, 4489–4498.
42 C. Huang, J. Zhou, S. Gu, P. Pan, Y. Hou, H. Xiong, T. Tang, Q. Wu and J. Wu, *ACS Appl. Mater. Interfaces*, 2023, **15**, 53242–53250.
43 J. Zhou, Q. Wu, P. Pan, H. Xiong, Y. Hou, Y. Chen, J. Wu and T. Tang, *ACS Appl. Bio Mater.*, 2024, **7**, 1694–1702.
44 C. Huang, Q. Wu, X. Li, P. Pan, S. Gu, T. Tang and J. Wu, *Biomacromolecules*, 2024, **25**, 4510–4522.
45 K. Kuciński and G. Hreczycho, *ChemSusChem*, 2017, **10**, 4695–4698.
46 G. D. Soraru, F. Babonneau, C. Gervais and N. Dallabona, *J. Sol-Gel Sci. Technol.*, 2000, **18**, 11–19.
47 M. G. Voronkov and V. N. Zgonnik, *Russ. J. Gen. Chem.*, 1957, **27**, 1476–1483.
48 K. A. Andrianov and L. M. Volkova, *Bull. Acad. Sci. USSR, Div. Chem. Sci.*, 1957, **6**, 317–322.
49 M. Tang, W. Wang, D. Xu and Z. Wang, *Ind. Eng. Chem. Res.*, 2016, **55**, 12582–12589.
50 D. Zhang, N. Jiang, X. Chen and B. He, *J. Appl. Polym. Sci.*, 2019, **137**, 48421.
51 Z. Liu, S. J. Picken and N. A. M. Besseling, *Macromolecules*, 2014, **47**, 4531–4537.
52 K. Liu, A. Pei, H. R. Lee, B. Kong, N. Liu, D. Lin, Y. Liu, C. Liu, P.-C. Hsu, Z. Bao and Y. Cui, *J. Am. Chem. Soc.*, 2017, **139**, 4815–4820.
53 C. Zhao, X. Gong, S. Wang, W. Jiang and S. Xuan, *Cell Rep. Phys. Sci.*, 2020, **1**, 100266.
54 W. Jiang, X. Gong, S. Wang, Q. Chen, H. Zhou, W. Jiang and S. Xuan, *Appl. Phys. Lett.*, 2014, **104**, 121915.
55 Y. Wang, S. Wang, C. Xu, S. Xuan, W. Jiang and X. Gong, *Compos. Sci. Technol.*, 2016, **127**, 169–176.
56 R. Cross, *Am. J. Phys.*, 2012, **80**, 870–875.
57 R. Cross, *Phys. Teach.*, 2012, **50**, 527–529.
58 N. Golinelli, A. Spaggiari and E. Dragoni, *J. Intell. Mater. Syst. Struct.*, 2015, **28**, 953–960.
59 Y. Wang, L. Ding, C. Zhao, S. Wang, S. Xuan, H. Jiang and X. Gong, *Compos. Sci. Technol.*, 2018, **168**, 303–311.
60 D. Zhang, N. Jiang, X. Chen and B. He, *J. Appl. Polym. Sci.*, 2020, **137**, 48421.
61 L. Zepeda-Velazquez, B. Macphail and M. A. Brook, *Polym. Chem.*, 2016, **7**, 4458–4466.
62 R. L. Vale, *J. Chem. Soc.*, 1960, 2252–2257.
63 Y. Zhang, C. Zang and Q. Jiao, *J. Phys.:Conf. Ser.*, 2020, **1637**, 012051.
64 S. Gao, Y. Liu, S. Feng and Z. Lu, *J. Polym. Sci., Part A: Polym. Chem.*, 2017, **55**, 2390–2396.
65 B. K. Teo and X. H. Sun, *Chem. Rev.*, 2007, **107**, 1454–1532.
66 N. Jiang, Z. Zhou, W. Xu, H. Ma and F. Ren, *Mater. Res. Express*, 2021, **8**, 065304.
67 B. Wei, R. Liu, G. Qi, G. Feng, Z. Li, Y. Zhang and H. Yan, *J. Vinyl Addit. Technol.*, 2024, **30**, 1025–1038.
68 Z. Zhou, H. Shen, F. Ren, H. Ma, W. Xu and S. Zhou, *J. Therm. Anal. Calorim.*, 2018, **132**, 1825–1831.
69 D. Gunes and B. Karagoz, *ACS Omega*, 2022, **7**, 43877–43882.
70 M. Tang, P. Zheng, K. Wang, Y. Qin, Y. Jiang, Y. Cheng, Z. Li and L. Wu, *J. Mater. Chem. A*, 2019, **7**, 27278–27288.
71 F. Tang, C. Dong, Z. Yang, Y. Kang, X. Huang, M. Li, Y. Chen, W. Cao, C. Huang, Y. Guo and Y. Wei, *Compos. Sci. Technol.*, 2022, **218**, 109190.

72 C. Xu, Y. Wang, J. Wu, S. Song, S. Cao, S. Xuan, W. Jiang and X. Gong, *Compos. Sci. Technol.*, 2017, **153**, 168–177.
73 M. Sang, J. Zhang, S. Liu, J. Zhou, Y. Wang, H. Deng, J. Li, J. Li, S. Xuan and X. Gong, *Chem. Eng. J.*, 2022, **440**, 135869.
74 T. Fan, S.-S. Xue, W.-B. Zhu, Y.-Y. Zhang, Y.-Q. Li, Z.-K. Chen, P. Huang and S.-Y. Fu, *ACS Appl. Mater. Interfaces*, 2022, **14**, 13778–13789.
75 T. Xing, K. Chen, Y. Wang, Z. Wu, Y. Xu and Y. Xu, *J. Appl. Polym. Sci.*, 2023, **140**, e54339.
76 A. Kurkin, V. Lipik, K. B. L. Tan, G. L. Seah, X. Zhang and A. I. Y. Tok, *Macromol. Mater. Eng.*, 2021, **306**, 2100360.
77 L. E. Porath and C. M. Evans, *Macromolecules*, 2021, **54**, 4782–4791.
78 N. Seetapan, A. Fuongfuchat, D. Sirikittikul and N. Limparyoon, *J. Polym. Res.*, 2013, **20**, 183.
79 Q. Chen, S. Li, X. Wang, S. Gao, J. Jin, E. Li, Y. Guo and F. Li, *Mater. Today Commun.*, 2023, **36**, 106638.
80 V. I. Mashchenko, N. N. Sitnikov, I. A. Khabibullina, D. N. Chausov, A. V. Shelyakov and V. V. Spiridonov, *Polym. Sci., Ser. A*, 2021, **63**, 91–99.
81 P. Qu, C. Lv, Y. Qi, L. Bai and J. Zheng, *ACS Appl. Mater. Interfaces*, 2021, **13**, 9043–9052.
82 C. A. D'Ambra, P. T. Getty, T. Eom, M. Czuczola, E. A. Murphy, S. Biswas, A. Abdilla, J. M. Mecca, T. D. Bekemeier, S. Swier, A. Fielitz, C. J. Hawker and C. M. Bates, *Chem. Mater.*, 2024, **36**, 5935–5942.
83 C. Chen, H.-F. Fei, J. J. Watkins and A. J. Crosby, *J. Mater. Chem. A*, 2022, **10**, 11667–11675.
84 P. Wang, L. Yang, M. Sun, Z. Yang, S. Guo, G. Gao, L. Xu, D. Ji, W. Cao and J. Zhu, *Macromol. Mater. Eng.*, 2021, **306**, 2000621.
85 P. Milkin, M. Danzer and L. Ionov, *Macromol. Rapid Commun.*, 2022, **43**, 2200307.
86 T. Wu and B. Chen, *ACS Appl. Mater. Interfaces*, 2016, **8**, 24071–24078.
87 Z. Zhao, H. Xie, D. Yang, Y. Wu, W. Tang, L. Zhu, W. Liu and T. Liu, *Polymer*, 2022, **254**, 125013.
88 S. Wang, S. Xuan, Y. Wang, C. Xu, Y. Mao, M. Liu, L. Bai, W. Jiang and X. Gong, *ACS Appl. Mater. Interfaces*, 2016, **8**, 4946–4954.
89 W. Lu, Q. Zhang, F. Qin, P. Xu, Q. Chen, H. Wang, F. Scarpa and H.-X. Peng, *Appl. Mater. Today*, 2021, **25**, 101222.
90 S. Wang, S. Xuan, M. Liu, L. Bai, S. Zhang, M. Sang, W. Jiang and X. Gong, *Soft Matter*, 2017, **13**, 2483–2491.
91 Q. Cheng, J. Lyu, N. Shi and X. Zhang, *Small Methods*, 2023, **7**, 2300002.
92 L. Shen, Q. Fu, K. Qian, K. Yu, H. Zhou, Y. Weng and Z. Zhang, *Mater. Des.*, 2020, **195**, 109039.
93 W. Wang, J. Zhou, S. Wang, F. Yuan, S. Liu, J. Zhang and X. Gong, *Nano Energy*, 2022, **91**, 106657.
94 Y. Chen, B. Dang, J. Fu, J. Zhang, H. Liang, Q. Sun, T. Zhai and H. Li, *ACS Nano*, 2022, **16**, 7525–7534.
95 J. Wu, Y. Wang, J. Zhang, C. Zhao, Z. Fan, Q. Shu, X. He, S. Xuan and X. Gong, *Matter*, 2022, **5**, 2265–2284.
96 T. Wu, E. Gray and B. Chen, *J. Mater. Chem. C*, 2018, **6**, 6200–6207.
97 P. Milkin, A. Zhanbassynova and L. Ionov, *Compos. Struct.*, 2024, **327**, 117709.
98 M. Sang, Y. Wu, S. Liu, L. Bai, S. Wang, W. Jiang, X. Gong and S. Xuan, *Composites, Part B*, 2021, **211**, 108669.
99 S. Liu, S. Wang, M. Sang, J. Zhou, T. Xuan, J. Zhang, S. Xuan and X. Gong, *Chem. Eng. J.*, 2023, **473**, 145214.
100 B. A. Patterson, M. H. Malakooti, J. Lin, A. Okorom and H. A. Sodano, *Compos. Sci. Technol.*, 2018, **161**, 92–99.
101 R. Nayak, I. Crouch, S. Kanesalingam, J. Ding, P. Tan, B. Lee, M. Miao, D. Ganga and L. Wang, *Text. Res. J.*, 2017, **88**, 812–832.
102 R. Nayak, I. Crouch, S. Kanesalingam, L. Wang, J. Ding, P. Tan, B. Lee, M. Miao, D. Ganga and R. Padhye, *Text. Res. J.*, 2018, **89**, 3411–3430.
103 P. Wu, J. Gu, X. Liu, Y. Ren, X. Mi, W. Zhan, X. Zhang, H. Wang, X. Ji, Z. Yue and J. Liang, *Adv. Mater.*, 2024, **36**, 2411131.
104 S. Zhang, L. Lu, S. Wang, F. Yuan, S. Xuan and X. Gong, *Composites, Part B*, 2021, **225**, 109268.
105 L. Gong, T. Xuan, S. Wang, H. Du and W. Li, *Nano Energy*, 2023, **109**, 108280.
106 S. Zhang, S. Wang, T. Hu, S. Xuan, H. Jiang and X. Gong, *Composites, Part B*, 2020, **180**, 107564.
107 S. Duan, M. Sang, H. Chen, Y. Pan, S. Liu, Z. Li, Z. Hu, Z. Zhang and X. Gong, *Adv. Funct. Mater.*, 2024, **34**, 2411821.
108 E. D'Elia, S. Barg, N. Ni, V. G. Rocha and E. Saiz, *Adv. Mater.*, 2015, **27**, 4788–4794.
109 J.-C. Lai, J.-F. Mei, X.-Y. Jia, C.-H. Li, X.-Z. You and Z. Bao, *Adv. Mater.*, 2016, **28**, 8277–8282.
110 K. Narumi, F. Qin, S. Liu, H.-Y. Cheng, J. Gu, Y. Kawahara, M. F. Islam and L. Yao, Proceedings of the 32nd Annual ACM Symposium on User Interface Software and Technology, 2019, 293–306.
111 Z. Lin, C. Chen, H. Huang, B. Xu, Y. Zhuang and R.-J. Xie, *Sci. China Mater.*, 2023, **66**, 4464–4472.
112 S. G. Patnaik, T. P. Jayakumar, Y. Sawamura and N. Matsumi, *ACS Appl. Energy Mater.*, 2021, **4**, 2241–2247.
113 M. Tang, Z. Li, K. Wang, Y. Jiang, M. Tian, Y. Qin, Y. Gong, Z. Li and L. Wu, *J. Mater. Chem. A*, 2022, **10**, 1750–1759.
114 M. Wójcik-Bania, A. Krowiak, J. Strzezik and M. Hasik, *Mater. Des.*, 2016, **96**, 171–179.
115 M. Zielecka, A. Rabajczyk, K. Cygańczuk, Ł. Pastuszka and L. Jurecki, *Materials*, 2020, **13**, 4785.
116 S. Hamdani, C. Longuet, D. Perrin, J.-M. Lopez-cuesta and F. Ganachaud, *Polym. Degrad. Stab.*, 2009, **94**, 465–495.
117 M.-F. Chen, Q. Zhou, L.-Z. Ni and G.-C. Wang, *J. Therm. Anal. Calorim.*, 2013, **114**, 1317–1324.
118 H. W. Bai, G. Wen, X. X. Huang, Z. X. Han, B. Zhong, Z. X. Hu and X. D. Zhang, *J. Eur. Ceram. Soc.*, 2011, **31**, 931–940.
119 J. Zhang, J. Liu, W. Gu, J. Sun, X. Gu, H. Li, J. Zhao and S. Zhang, *Composites, Part A*, 2024, **187**, 108505.

120 G. Camino, S. M. Lomakin and M. Lageard, *Polymer*, 2002, **43**, 2011–2015.
121 Y. Wan, S. Yu, S. Jiang, Q. Pei, S. Xu, W. Cao, X. Liu and Y. Lan, *J. Anal. Appl. Pyrolysis*, 2021, **158**, 105274.
122 D. G. Hall, *Boronic Acids*, 2005, pp. 1–99.
123 Y. Li, L. Du, P. Zhu and Z. Jiang, *Prog. Org. Coat.*, 2024, **197**, 108861.
124 L. Zhang, Y. Xia, J. Sun, Z. Guo, Z. Fang, P. Chen and J. Li, *Prog. Org. Coat.*, 2024, **188**, 108219.
125 Y. Zhu, R. Yu, S. Wang, H. Xing, J. Qiu, J. Liu and T. Tang, *Chem. Eng. J.*, 2022, **446**, 136742.
126 Z. Liu, M. Ma, B. Ge, Y. Zheng, S. Chen, Y. Shi, H. He, Y. Zhu and X. Wang, *Chem. Eng. J.*, 2023, **474**, 145799.
127 Z. Zeng, H. Jin, M. Chen, W. Li, L. Zhou and Z. Zhang, *Adv. Funct. Mater.*, 2016, **26**, 303–310.
128 Z. Zhou, C. You, Y. Chen, W. Xia, N. Tian, Y. Li and C. Wang, *Org. Electron.*, 2022, **105**, 106491.
129 S. Wang, F. Yuan, S. Liu, J. Zhou, S. Xuan, Y. Wang and X. Gong, *J. Mater. Chem. C*, 2020, **8**, 3715–3723.
130 Y. Chen, X. Pu, M. Liu, S. Kuang, P. Zhang, Q. Hua, Z. Cong, W. Guo, W. Hu and Z. L. Wang, *ACS Nano*, 2019, **13**, 8936–8945.
131 D. Wang, J. Zhang, G. Ma, Y. Fang, L. Liu, J. Wang, T. Sun, C. Zhang, X. Meng, K. Wang, Z. Han, S. Niu and L. Ren, *ACS Nano*, 2021, **15**, 19629–19639.
132 C. Zhao, Y. Wang, L. Gao, Y. Xu, Z. Fan, X. Liu, Y. Ni, S. Xuan, H. Deng and X. Gong, *ACS Appl. Mater. Interfaces*, 2022, **14**, 21564–21576.
133 C. Wan, Z. Feng, Y. Gao, J. Yu, Z. Wu, Z. Yang, S. Mao, R. Guo, W. Huo and X. Huang, *ACS Sens.*, 2024, **9**, 5253–5263.
134 C.-T. Kuo, Y.-C. Lin, K.-Y. Tu and L.-H. Hu, *J. Mater. Chem. A*, 2024, **12**, 15608–15618.
135 S. Wang, L. Gong, Z. Shang, L. Ding, G. Yin, W. Jiang, X. Gong and S. Xuan, *Adv. Funct. Mater.*, 2018, **28**, 1707538.
136 X. Hong, Y. Zhao, C. Gong, J. Chao, B. Lv, Z. Xu, L. Xu and W. Zheng, *ACS Appl. Nano Mater.*, 2023, **6**, 7543–7552.
137 L. A. Bloomfield, *arXiv*, 2018, preprint, arXiv:1801.09253, DOI: **10.48550/arXiv.1801.09253**.